Anoctamin-1 is induced by TGF-beta and contributes to lung myofibroblast differentiation.

Eleanor B. Reed[1], Shaina Orbeta[2], Albert Sitikov[1], Irena Levitan[3], Gökhan M. Mutlu[1], Alexander A. Mongin[2,&], Nickolai O. Dulin[1,&,*].

[1]Department of Medicine, Section of Pulmonary and Critical Care Medicine, The University of Chicago, Chicago, IL, USA. [2]Department of Neuroscience & Experimental Therapeutics, Albany Medical College, Albany, NY. [3]Departments of Medicine, Pharmacology and Bioengineering, University of Illinois at Chicago, Chicago, IL.

[&] Co-senior authors.

*** To whom correspondence should be addressed:** Nickolai O. Dulin, The University of Chicago Department of Medicine, Section of Pulmonary and Critical Care Medicine, 5841 S. Maryland Ave, MC6076, Chicago, IL 60637.

Email: ndulin@bsd.uchicago.edu

Running Title: Control of myofibroblast differentiation by anoctamin-1.

Funding: This study was supported by NHLBI Award R01 HL149993 (to NOD) and NINDS Award R01 NS111943 (to AAM).

Abstract

Idiopathic pulmonary fibrosis (IPF) is a devastating disease characterized by progressive scarring of the lungs and resulting in deterioration in lung function. Several profibrotic factors drive pulmonary fibrosis, with transforming growth factor-beta (TGF-beta) being the most established. TGF-beta promotes transformation of tissue fibroblasts to myofibroblasts, a key finding in the pathogenesis of pulmonary fibrosis. Anoctamin-1 (ANO1), also known as TMEM16A, is a calcium-activated chloride channel. We found that TGF-beta robustly upregulates ANO1 expression in human lung fibroblasts (HLF) at mRNA and protein levels. Consistent, ANO1 was readily detected in fibrotic areas of IPF lungs. TGF-beta treatment of HLF resulted in a significant increase in steady state accumulation of intracellular chloride concentration, which was prevented by a specific ANO1 inhibitor, $T16A_{inh}$-A01, or by siRNA-mediated *ANO1* knockdown. $T16A_{inh}$-A01 or *ANO1* siRNA significantly inhibited TGF-beta-induced myofibroblast differentiation as determined by the expression of smooth muscle alpha-actin, collagen-1 and fibronectin. Mechanistically, pharmacological or knockdown-mediated inhibition of ANO1 did not have an effect on the initial TGF-beta signaling (Smad2 phosphorylation), but it blocked downstream TGF-beta signaling including Rho pathway (assessed by phosphorylation of myosin light chain) and AKT activation. Together, these data demonstrate that ANO1 is a TGF-beta-inducible chloride channel that largely contributes to the increase in intracellular chloride concentration in TGF-beta-treated cells. Furthermore, ANO1 mediates TGF-beta-induced myofibroblast differntiation, at least partially through activation of Rho pathway and of AKT.

Keywords: Anoctamin-1; myofibroblast; TGF-beta; chloride channel; fibrosis.

New & Noteworthy.

Pulmonary fibrosis is a devastating disease characterized by progressive scarring of the lungs and resulting in deterioration of lung function. Myofibroblasts are cells produced from tissue fibroblasts during this disease and are the key pathologic cells that contribute to lung scaring. Transforming growth factor-beta (TGF-beta) is the cytokine that drives myofibroblast differentiation. This study identifies a novel role of a chloride channel, Anoctamin-1, in the cellular mechanism TGF-beta-induced myofibroblast differentiation.

Introduction.

Idiopathic pulmonary fibrosis (IPF) is a progressive, fatal disease characterized by parenchymal fibrosis and structural distortion of the lungs. Age-adjusted mortality due to pulmonary fibrosis is increasing (1), and it poses a vexing clinical challenge given the lack of effective therapy. IPF is a disorder of abnormal wound healing (2, 3), wherein the initial trigger is injury to the alveolar epithelial cell, followed by a non-resolving wound-healing response (4-6). Migration of interstitial fibroblasts to the sites of injury and their differentiation to myofibroblasts are thought to be critical processes in pathogenesis of pulmonary fibrosis. Myofibroblasts are responsible for secretion of extracellular matrix proteins and pro-fibrotic factors (7, 8), thus perpetuating ongoing tissue remodeling and fibrosis. Myofibroblasts are invariably found in histologic sections of human lung specimens from IPF patients and are thought to be a critical pathogenic mechanism responsible for the progressive nature of IPF.

Transforming Growth Factor-β (TGFβ-) is the most established known driver of myofibroblast differentiation (9-11). TGF-β has been localized to areas of fibrosis in both experimental pulmonary fibrosis and in human disease (9, 12, 13). Lung-targeted overexpression of TGF-β results in the development of lung fibrosis in animals (11, 14). Conversely, inhibition of TGF-β via soluble TGF-β receptors can inhibit in vivo fibrogenesis (15, 16).

TGF-β signals through transmembrane-receptor serine/threonine kinases that phosphorylate Smad transcription factors (Smad2/3), leading to their heteromerization with a common mediator Smad4, nuclear translocation of Smad2/3/4 complex and activation of transcription of TGF-β target genes (7, 17, 18). We and others have established that signaling

downstream of Smad-dependent gene transcription is critical for myofibroblast differentiation; this partially includes TGF-β -induced RhoA/SRF pathway (19-21) and AKT activation (22-24).

Anoctamine-1 (ANO1), also known as TMEM16A, DOG1 (Discovered On Gastrointestinal stromal tumors 1), ORAOV2 (ORAl cancer OVerexpressed), and TAOS-2 (Tumor Amplified and Overexpressed) was initially found to be overexpressed in a number of cancer tissues and is thought to contribute to cancer cell growth and tumorigenesis (25, 26). Subsequently, ANO1 was identified as calcium-activated chloride channel (27-29). The most recognized cellular functions of ANO1 include the control of cancer cell proliferation, survival and migration by ANO1 (25, 26), secretory function of ANO1 in the epithelia, such as airways, intestines, salivary glands, renal tubules and sweat glands (30), induction of electrical pacemaker activity of interstitial cells of Cajal in gastrointestinal smooth muscles (31), control of acute pain sensation, chronic pain and anxiety-related behaviors (32, 33), and contribution to contraction of airway and vascular smooth muscles (32). Through an unbiased microarray analysis, we identified ANO1 as one of the top transcripts induced by TGF-β in primary cultured human lung fibroblasts (HLF), which was not previously recognized. We therefore sought to confirm this finding by appropriate biochemical approaches and examine the role of ANO1 in a control of intracellular chloride homeostasis and myofibroblast differentiation.

Materials and Methods.

Primary culture of human lung fibroblasts (HLF). Human lung fibroblasts (HLF) were isolated from human lungs rejected for transplantation through the Regional Organ Bank of Illinois (ROBI) / Gift of Hope. Human lung tissue samples were placed in DMEM with antibiotics. Lung tissue was minced to ~1 mm^3 pieces, washed, and plated on 10-cm plates in growth media containing DMEM supplemented with 10% FBS and antibiotics. The media was changed twice a week. After approximately 2 weeks, the explanted and amplified fibroblasts were trypsinized, cleared from tissue pieces by sedimentation, and further amplified as passage 1. Unless indicated, cells were grown in 12-well plates at a density of $1x10^5$ cells per well in a growth media for 24 hours, starved in DMEM containing 0.1% FBS for 48 hours (48-hour starvation is important to ensure a quiescence in all cells), and treated with desired drugs for various times as indicated in the figure legends. Primary cultures were used from passage 3 to 8.

Immunohistochemistry. Fibrotic lungs from IPF patients were obtained shortly after lung transplantation at the University of Chicago under the IRB protocol #14514A. Lung tissues were fixed in formalin, washed in 70% ethanol and paraffin embedded. Lung sections were stained with control IgG or ANO1 antibodies (Abcam # ab53212) by the University of Chicago Immunohistochemistry Core Facility.

siRNA transfection. HLF were plated at a density of 0.8 $x10^5$ cells per well (12-well plates, for western blotting), or 1.6 $x10^5$ cells per well (6-well plates, for real time qPCR) and grown for 24 hours. Cells were then transfected with 10 nM control or ANO1 siRNA using Lipofectamine RNAiMAX Reagent (thermo Fisher Scientific, Waltham, MA) according to the standard

protocol and kept in growth media for additional 24 hours, followed by serum starvation in 0.1% FBS for 48 hours, and then treatment with TGF-β for desired times.

Real-time qPCR. Direct-Zol RNA mini prep kit (Zymo Research, Irvin, CA) was used to isolate total RNA following the manufacturer's protocol. RNA was random primed reverse transcribed using iScript cDNA synthesis kit (Bio-Rad, Hercules, CA) according to the manufacturer's protocols. Real-time PCR analysis was performed using iTaq SYBR Green supermix with ROX (Bio-Rad) in a MyIQ single-color real-time PCR detection system (Bio-Rad). The ANO1 primers were: GCAGAGAGGCCGAGTTTCTG (forward) and GCTCAGCCACTTTGGGCTG (reverse).

Western blotting. Cells were lysed in the urea buffer containing 8 M deionized urea, 1% SDS, 10% glycerol, 60mM Tris-HCl, pH 6.8, 0.02% pyronin Y, and 5% β-mercaptoethanol. Lysates were sonicated for 5 seconds. Samples were then subjected to polyacrylamide gel electrophoresis and Western blotting with desired primary antibodies and corresponding horseradish peroxidase (HRP)-conjugated secondary antibodies, and developed by chemiluminescence reaction (Pierce/Thermo Fisher Scientific). Digital chemiluminescent images below the saturation level were obtained with a LAS-4000 analyzer, and the light intensity was quantified using Multi Gauge software (Fujifilm, Valhalla, NY).

Measurements of intracellular chloride. Intracellular chloride levels ($[Cl^-]_i$) were determined using steady-state $^{36}Cl^-$ accumulation, which is proportional to $[Cl^-]_i$ and can be converted to cytosolic concentration values if the precise volume of intracellular water is known (34, 35). HLF were replated into 6-well plates, grown in DMEM-FBS, and subsequently differentiated and treated as described above. On the day of assay, cells were additionally pretreated with ion

transport inhibitors (concentrations and timing are specified in Results). $^{36}Cl^-$ accumulation was initiated by adding to each well 1/10 volume of the low-FBS assay medium containing 0.5 µCi/ml $Na^{36}Cl$ (American radiolabeled Chemicals, St. Louis, MO) and 10 mM HEPES (final concentrations). HEPES was supplemented to minimize alkalinization during temporary removal of cells from CO_2 incubator. $^{36}Cl^-$ accumulation was carried out for 30 min at 37ºC in CO_2 incubator. The radioisotope uptake was terminated by aspirating $^{36}Cl^-$-containing medium and four immediate washes with 2 ml of ice-cold medium containing (in mM) 300 mannitol, 3 $MgSO_4$, 10 HEPES (pH 7.4). After the final wash, HLF were lysed in 1 ml of solution containing 2% SDS plus 8 mM EDTA. Half of each cell lysate sample was used for [^{36}Cl] detection, while the second half was utilized for determining protein levels in individual wells. $^{36}Cl^-$ in each sample was counted with a TriCarb 4910 scintillation counter (Perkin Elmer, Waltham, MA) after adding an Ecoscint A scintillation cocktail (National Diagnostics, Atlanta, GA). The $[Cl^-]_i$ values were quantified by normalizing $^{36}Cl^-$ counts to specific $^{36}Cl^-$ activity and either protein levels or cell numbers in each individual well (see Results).

Materials. TGFβ was from EMD Millipore (catalog # GF111). The following antibodies for Western blotting were from Millipore-Sigma: smooth muscle α-actin (catalog # A5228), β-actin (catalog # A5441), α-tubulin (catalog # T6074) and myosin light chain (catalog # M4401). Antibodies against human collagen-1A1 (catalog # sc-28657) and AKT (catalog # sc-8312) were from Santa Cruz Biotechnology (Dallas, TX). Antibodies against ANO1 (catalog # 14476), Smad2 (catalog # L1603), phospho-Smad2 (catalog # 13804), P-MLC (catalog # 3671) and P-AKT (catalog # 9271) from Cell Signaling Technology (Danvers, MA). Additionally, we used ANO1 antibodies for immunohistochemistry from Abcam (Cambridge, UK, catalog # ab53212). $T16A_{inh}$-A01 inhibitor was from Calbiochem (la Jolla, CA). ANO1 siRNA (catalog # 1027417)

and control siRNA (catalog # 1027281) were from Qiagen. $Na^{36}Cl$ (0.1 mCi/ml, 16 mCi/g Cl) was from American Radiolabeled Chemicals (St. Louis, MO).

Statistical Analysis. All data are presented as mean values +SD. Normally distributed data were analyzed using Student t-test or one-way ANOVA with the Tukey honest significant difference test post hoc correction for multiple comparisons, as appropriate. Normalized-to-controls and non-normally distributed data were analyzed using Kruskal-Wallis non-parametric test followed by Dunn's post hoc correction for multiple comparisons. For data sets presented in Fig. 3 and 4, we performed additional preplanned analysis exploring the effect of ANO1 inhibitor and ANO1 siRNA in TGFβ-treated cells. The latter analysis was conducted using a one-population t-test with values compared to 100%. Values of $p<0.05$ were considered statistically significant. All statistical analyses were performed in Prism v. 9.5 (GraphPad Software, Boston, MA),

Results.

Expression of ANO1 in human lung myofibroblasts in cell culture and in human lung fibrotic tissues

Treatment of primary cultured human lung fibroblasts (HLF) with TGF-β resulted in a robust accumulation of ANO1 expression at mRNA and protein levels, as assessed by real time qPCR and western blotting (Figs. 1A, 1B, respectively). Given that myofibroblasts are the significant contributors to tissue scaring during fibrotic processes, we assessed the expression of ANO1 in the lung explants from patients with idiopathic pulmonary fibrosis (IPF). As shown in figure 1C, ANO1 expression was clearly observed in fibrotic areas of the lungs of IPF patients, albeit with a patchy appearance (Fig. 1C).

Effect of TGF-β on intracellular chloride levels, and the role of ANO1 in HLF

Given that ANO1 is a chloride channel, we then asked how TGFβ affects intracellular chloride homeostasis, and the role of ANO1, using previously developed approach of measuring the steady state accumulation of $^{36}Cl^{-}$ inside the cells. Equilibrium of $^{36}Cl^{-}$accumulation is directly proportional to intracellular chloride levels ($[Cl]_i$) and it can be converted to cytosolic concentration values if the precise volume of intracellular water is known (34, 35). To determine appropriate conditions for measuring steady state $^{36}Cl^{-}$ accumulation, we first assessed the kinetics of $^{36}Cl^{-}$ uptake in HLF. As shown in Fig. 2A, intracellular $^{36}Cl^{-}$levels reached equilibrium after approximately 10-15 min. The fast equilibration was determined by $^{36}Cl^{-}$ uptake through several ion transport systems. Addition of the inhibitor of Na^{+}-K^{+}-$2Cl^{-}$ cotransporter (NKCC1), bumetanide, reduced steady-state chloride accumulation by ~25% (n=4, $p<0.05$, data not shown). When we combined bumetanide with the anion exchanger blocker

DIDS (4,4′-Diisothiocyano-2,2′-stilbenedisulfonic acid), the $^{36}Cl^-$ uptake values were reduced by >90% and failed to saturate within 30 min (Fig. 2A). These results indicate that the main transport system that equilibrates $^{36}Cl^-$ across the plasma membrane of HLFs is the DIDS-sensitive chloride-bicarbonate exchanger, with additional contributions of NKCC1 and possibly DIDS-sensitive Cl^- channels. This is consistent with the pervious publications in human skin fibroblasts (36).

We next examined the effect of TGF-β and the pharmacological inhibitor of ANO1, $T16A_{inh}$-A01 (37), on intracellular chloride levels in HLF. As shown in figure 2B, a 48-hr treatment of HLF with TGF-β resulted in a significant increase in a steady state $^{36}Cl^-$ accumulation in HLF. Further, $T16A_{inh}$-A01 significantly suppressed both the basal and TGF-β-induced steady state $^{36}Cl^-$ accumulation in HLF. We then used siRNA approach to knock down ANO1 in HLF. TGF-β increased $^{36}Cl^-$ accumulation in cells treated with control siRNA; and similarly to T16Ainh-A01, ANO1 knockdown completely blunted TGF-β-induced accumulation of intracellular $^{36}Cl^-$, although intracellular $^{36}Cl^-$ levels under the basal conditions were not affected by siANO1 (Fig. 2C). The successful knockdown of ANO1 in HLF is demonstrated in Fig. 3B. Together, these data suggest that TGF-β-induced increase in intracellular Cl^- ($^{36}Cl^-$) is fully determined by the increased expression of ANO1.

Role of ANO1 in TGF-β-induced myofibroblast differentiation

As shown in Figure 3, treatment of HLF with TGF-β for 48 hours resulted in differentiation to myofibroblasts as defined by a profound increase in the expression of the extracellular matrix proteins, collagen-1 (Col1A1, Fig. 3A2) and fibronectin (FN, Fig. 3A3), and dramatic increase in the cellular smooth muscle α-actin (α-SMA, Fig. 3A4). Pretreatment of HLF with ANO1

inhibitor T16A$_{inh}$-A01 blocked the TGF-β-induced increase in ANO1 levels (Fig. 3A1), but equally importantly blunted the TGF-β-induced upregulation of α-SMA, Col1A1 and FN without affecting the levels of house-keeping β-actin protein (Fig. 3A2-4). The effect of T16A$_{inh}$-A01 on the TGF-β-induced increase in ANO1 levels (Fig. 3A), suggests that in addition to pharmacological inhibition, long-term T16A$_{inh}$-A01 treatment also affects the expression of ANO1 via yet unknown mechanism. To corroborate the results with pharmacological inhibition of ANO1, we used siRNA approach. Figure 3B shows the efficient ANO1 protein knockdown by ANO1 siRNA and a very similar to T16A$_{inh}$-A01 significant decrease in TGF-β-induced expression of α-SMA, Col1A1 and FN (Figs. 3B2-4).

Control of TGF-β-induced signaling by ANO1 in HLF.

We next began exploring the mechanism through which ANO1 controls the TGF-β-induced myofibroblast differentiation. Phosphorylation of Smad2/3 transcription factors by TGF-β receptors is the proximal event in TGF-β signaling. As shown in Figure 4A (P-Smad2 blot), a 30-minute treatment of HLF with TGF-β resulted in phosphorylation of Smad2 without affecting the total levels of Smad2. Pretreatment of HLF with ANO1 inhibitor T16A$_{inh}$-A01 had no effect on TGF-β-induced Smad2 phosphorylation (Fig. 4A), suggesting that the initial signaling event is not affected. We next focused on the downstream, delayed signaling processes that are required for myofibroblast differentiation in response to TGF-β. We and others have discovered previously that the downstream, delayed signaling processes involves Rho-mediated signaling (19-21). We assessed changes in this pathway by measuring phosphorylation state of myosin light chain (MLC), which is controlled by Rho-mediated signaling (38) and represents a widely used indirect assay for Rho pathway activation (39, 40). A 48-hr treatment of HLF with TGF-β resulted in a >5-fold increase in phosphorylation of MLC, and this effect was significantly

inhibited by pharmacological inhibitor of ANO1, T16A_{inh}-A01, whereas the total MLC levels remained unchanged. (Fig. 4A1). We also examined in HLF the role of ANO1 in a control of AKT phosphorylation, which has been reported in other cells (41, 42), albeit not in the context of TGF-β. Treatment of HLF with TGF-β for 48 hours resulted in a significant AKT phosphorylation; and this effect was inhibited by T16A_{inh}-A01 (Fig. 4A2). Finally, to corroborate the data obtained with pharmacological ANO1 inhibitor, we used the ANO1 knockdown approach. Similarly to T16A_{inh}-A01, ANO1 siRNA had no significant effect on Smad2 phosphorylation, but it completely abolished TGF-β-induced phosphorylation of MLC and AKT (Fig. 4B1-B2).

Discussion.

This study describes the following novel findings. (i) ANO1 is abundant in fibrotic areas of the IPF lung, and the expression of ANO1 is robustly induced by TGF-β in cultured HLF. (ii) TGFβ increases the intracellular Cl^- levels in HLF, and this effect is fully determined by the increased expression of ANO1 (because it is ablated by both ANO1 inhibitor or ANO1 siRNA). (iii) ANO1 expression is critical for TGF-β-induced myofibroblast differentiation based on the ANO1-depenndent expression of several myofibroblast markers. (iv) ANO1 controls TGF-β-stimulated activation of Rho and AKT signaling pathways in HLF, both of which have been implicated in myofibroblast differentiation.

We have previously reviewed the published data on the regulation of ANO1 expression under various conditions in a variety of cells (43). It was reported that ANO1 expression can be induced by several cytokines from the interleukin family (e.g., IL-4, IL-6, IL-13), lysophosphatidic acid, and epidermal growth factor in various cell types. The controversial (possibly cell-specific) effects on ANO1 expression (up or down) were also reported for G protein coupled receptor agonist, angiotensin II, and for serum (reviewed in (43)). To our knowledge, this study represents the first demonstration of a robust induction of ANO1 expression by TGF-β at both mRNA and protein levels in lung human lung fibroblasts (Fig. 1). The generality of the effect of TGF-β on ANO1 expression in various cell types requires further investigation.

The mechanism of TGF-β-induced ANO1 expression in HLF requires further investigation, but a number of possibilities can be deducted from the existing literature. (i) ANO1 promoter may have previously unrecognized SMAD-binding elements. (ii) ANO1

transcription may be indirectly induced by signaling pathways downstream of Smad-dependent gene transcription. For example, ANO1 expression is induced by IL-6 (through STAT3 transcription factor) in pancreatic acinar cells (44); IL-6 expression is induced by TGF-β in HLF (45); TGF-β recruits Smad3 for myofibroblast differentiation (46), altogether suggesting TGFβ/SMAD and/or IL-6/STAT3 pathway for ANO1 expression. (iii) On the other hand, ANO1 transcription was reported to be driven by myocardin/serum response factor (SRF) transcription factors in vascular smooth muscle cells (47). Given our previous findings establishing SMAD-dependent activation of Rho/SRF pathway by TGF-β in HLF (20, 21), SRF-dependent transcription of ANO1 in response to TGF-β is also plausible. Furthermore, as discussed below, the Rho/SRF pathway may provide a positive feedback loop in the mechanism of myofibroblast differentiation, given that ANO1 mediates TGF-β-induced Rho signaling (indirectly determined by measuring MLC phosphorylation in this study) in HLF (Fig. 4).

Another major phenomenon that we observed in all performed experiments is a strong increase in the intracellular Cl^- levels in HLF upon treatment with TGF-β (Fig. 2). Thus, upregulation of plasmalemmal ANO1 appears to elevate $[Cl^-]_i$, superficially suggesting that ANO1 is responsible for Cl^- accumulation in this cell type. Pharmacological and knockdown experiments are consistent with this idea but paint a nuanced picture. The ANO1 blocker, $T16A_{inh}$-A01, strongly reduced intracellular Cl^- levels under both basal and TGF-β-induced conditions (Fig. 2B). ANO1 downregulation using siRNA prevented TGF-β effect on the intracellular $[C_l^-]_i$ but did not modify baseline $[Cl^-]_i$ on its own (Fig. 2C). Partial discrepancy between effects of the two treatments on baseline $[Cl^-]_i$ may due to the limited specificity of T16Ainh-A01. In one study, T16Ainh-A01 has been found to block the ubiquitously expressed volume-regulated anion channels encoded by LRRC8 proteins with the IC_{50} value of ~5 μM

(48). Inhibition of the LRRC8 anion channels, alone or in combination with the block of ANO1, can hyperpolarize HLF by reducing persistent loss of negatively charged Cl^- from the cytosol and in such a way indirectly reduce steady state $^{36}Cl^-$ accumulation. The precedents for such an idea have been established in smooth muscle cells (49). In this latter model, the primary effects of ANO1 on TGF-β-induced cell transformation may be mediated by changes in membrane potential, rather than in change in the $[Cl^-]_i$, which is a future direction of our studies.

Another important finding of this study is that pharmacological or knockdown-mediated inhibition of ANO1 significantly attenuates TGF-β-induced myofibroblast differentiation of HLF (Fig. 3). In mechanistic studies, our data suggest that inhibition of ANO1 does not affect immediate TGF-β signaling (Smad2 phosphorylation), but it blocks downstream signaling – TGF-β-induced phosphorylation of MLC and AKT (Fig. 4). Phosphorylation of MLC (controlled by Rho-dependent inactivation of MLC phosphatase (38)) has been commonly used for an indirect assessment of Rho activation (39, 40). Considering our previous findings of the critical role of Rho/SRF pathway in TGF-β-induced myofibroblast differentiation (19-21), and given the results of this study showing a complete inhibition of MLC phosphorylation by pharmacological or knockdown-mediated inhibition of ANO1 (Fig. 4), we argue that the Rho/SRF pathway could be one of the mechanisms by which ANO1 controls myofibroblast differentiation in response to TGF-β. On the other hand, ANO1 transcription has been reported to be driven by SRF (47), potentially suggesting a positive feed-forward loop mechanism through SRF/ANO1- driven myofibroblast differentiation. We also demonstrated that inhibition of ANO1 blocks TGF-β-induced phosphorylation of AKT (Fig. 4). The role of ANO1 in AKT phosphorylation has been reported in other cells (41, 42), but not in the context of TGF-β stimulation. AKT plays an

important role in TGF-β-induced myofibroblast differentiation (24) and may mediate the pro-fibrotic function of ANO1.

Our finding of the contributions of ANO1 to myofibroblast transformation *in vitro* are likely important for understanding pathophysiology of IPF but also raise a number of new fundamental and translational questions relevant to ANO1. (i) The contribution of ANO1 to a fibrotic process in the lung should be investigated in future *in vivo* experiments. (ii) The mechanism of TGF-β-induced ANO1 expression in fibroblasts is interesting on its own and needs to be further explored, including the role for intracellular chloride in control of this process.

Acknowledgements.

This study was supported by NHLBI Award R01 HL149993 (to NOD) and NINDS Award R01 NS111943 (to AAM).

Figure legends.

Figure 1. Expression of ANO1 in human lung myofibroblasts and in fibrotic areas of human lungs with idiopathic pulmonary fibrosis (IPF). A-B, Confluent human lung fibroblasts (HLF) were serum starved in 0.1% FBS for 48 hr, followed by treatment with TGF-β (1 ng/ml) for indicated times. **A,** ANO1 mRNA expression as determined by RT-qPCR. Data are the mean values ±SD. ***p<0.001, t-test. **B,** Representative image and quantitation of ANO1 protein expression as determined by western blot analysis. Data are the normalized to control mean immunoreactivity values ±SD. *, p<0.05, ***p<0.001, Kruskal-Wallis non-parametric test with Dunn's correction for multiple comparisons**. C,** Immunohistochemical staining of fibrotic areas of human IPF lung sequential sections with ANO1 antibodies as compared to the IgG control. Shown are representative IHC images from three IPF lungs.

Figure 2. Effect of TGF-β on and the role of ANO1 in a control of intracellular Cl^- levels in human lung fibroblasts (HLF). A, Kinetics of Cl^- accumulation in HLF. Cl^- uptake was measured as radiotracer accumulation after adding $^{36}Cl^-$ into cell culture medium. Serum-starved (for 48 hr) HLF cells were pretreated for 30 min with either vehicle or combination of 1 mM DIDS plus 20 µM bumetanide. The same inhibitors were present in transport assay media. Data are the mean values ±SD in three experiments. ****p<0.0001, repeated measures ANOVA; inhibitors vs. control. **B,** Effect of the ANO1 inhibitor, T16Ainh-A01 (T16Ai), on intracellular Cl^- levels in control and TGF-β-treated HLF. Intracellular Cl^- levels were measured as the steady state $^{36}Cl^-$ accumulation and normalized to the number of cells per well as described in methods. 30 µM T16Ainh-A01 was added for 1 h before and during $^{36}Cl^-$ transport assay. Data represent the mean values ±SD from seven independent experiments in two HLF passages. *p<0.01, **p<0.01; ***p<0.001; One-way ANOVA with Tukey post hoc correction

for multiple comparisons. **C,** The effect of siRNA-mediated ANO1 knockdown on intracellular Cl^- levels in control and TGFβ-treated primary human lung fibroblasts. HLF cells were treated with the siRNA targeting ANO1 (siANO1) or the negative control siRNA (siCont), and TGF-β or vehicle control for 48hr as described in Methods. The steady-state $^{36}Cl^-$ accumulation was measured and normalized as in panel B. Data represent the mean values ±SE of eight independent experiments performed in two HLF passages. **p<0.01, ***p<0.001, One-way ANOVA with Tukey post hoc correction for multiple comparisons.

Figure 3. Role of ANO1 in TGFβ-induced myofibroblast differentiation. A, Representative image and quantification of western blot analysis of the effect of the pharmacological inhibitor of ANO1, $T16A_{inh}$-A01 (T16Ai) on myofibroblast differentiation. Serum-starved (48 hr) HLF were pretreated with the T16Ai for 1hr, followed by treatment with TGF-β (1 ng/ml) for 48 hr. Cell lysates were then probed for immunoreactivity of anactomin-1 (ANO1, A1), collagen 1A1 (Col1A1, A2), fibronectin (FN, A3), and smooth muscle α-actin (SMA, A4). Data are the mean values ± SD. *p<0.05, **p<0.01, ***p<0.001, Kruskal-Wallis with Dunn's post hoc correction vs. TGFβ group. Brace brackets and $^{\#\#\#}$p<0.001; $^{\#\#\#\#}$, p<0.0001, preplanned comparison of TGF-β effect with and without ANO1 inhibitor. **B**, Representative image and quantification of western blot analysis of the effect of siRNA targeting ANO1 on myofibroblast transformation. Serum-starved (48 hr) HLF were treated with ANO1 siRNA followed by treatment with TGF-β (1 ng/ml) for 48 hr. Cell lysates were then probed for immunoreactivity of anactomin-1 (ANO1, B1), collagen 1A1 (Col1A1, B2), fibronectin (FN, B3), and smooth muscle α-actin (SMA, B4). Data are the mean values ±SD. *p<0.05, **p<0.01, ***p<0.001, Kruskal-Wallis with Dunn's post hoc correction vs. TGF-β group. Brace brackets and $^{\#\#}$p<0.01; $^{\#\#\#}$p<0.001; $^{\#\#\#\#}$, p<0.0001, preplanned comparison of TGF-β effect with and without ANO1 siRNA.

Figure 4. ANO1 controls TGFβ-induced signaling in HLF. A, Representative images and quantification of western blot analysis of the effect of the pharmacological inhibitor of ANO1, T16Ainh-A01 (T16Ai) on intracellular signaling in HLF. Serum-starved (48 hr) cells were pretreated for 1 hr with T16Ai followed by treatment with TGF-β (1 ng/ml) for 30 minutes (P-Smad2, Smad2), or for 48hr (P-MLC, MLC, P-AKT, AKT). Data represent the mean values of P-MLC (**A1**) and P-AKT (**A2**) immunoreactivity normalized to TGF-β group. *p<0.05, **p<0.01, Kruskal-Wallis with Dunn's post hoc correction vs. TGF-β group. #p<0.05; ##, p<0.01, preplanned comparison of TGF-β effect with and without T16Ai. **B,** Representative images and quantification of western blot analysis of the effect of siRNA targeting ANO1, (siANO1) and nonsense control siRNA (siCont) on intracellular signaling in HLF. Cells were transfected with siCont or siANO1, serum-starved (48 hr), followed by treatment with TGF-β (1 ng/ml) for 30 minutes (P-Smad2, Smad2), or for 48hr (P-MLC, MLC, P-AKT, AKT). Data represent the mean values of P-MLC (**B1**) and P-AKT (**B2**) immunoreactivity normalized to TGF-β group. *p<0.05, **p<0.01, 888p<0.001, ****p<0.0001, Kruskal-Wallis with Dunn's post hoc correction vs. TGF-β group. ###p<0.001, ####p<0.01, preplanned comparison of TGF-β effect with and without siANO1.

References.

1. Olson AL, Swigris JJ, Lezotte DC, Norris JM, Wilson CG, Brown KK. Mortality from pulmonary fibrosis increased in the United States from 1992 to 2003. *Am J Respir Crit Care Med* 2007; 176: 277-284.
2. White ES, Lazar MH, Thannickal VJ. Pathogenetic mechanisms in usual interstitial pneumonia/idiopathic pulmonary fibrosis. *J Pathol* 2003; 201: 343-354.
3. Hardie WD, Glasser SW, Hagood JS. Emerging concepts in the pathogenesis of lung fibrosis. *Am J Pathol* 2009; 175: 3-16.
4. Noble PW, Homer RJ. Back to the future: historical perspective on the pathogenesis of idiopathic pulmonary fibrosis. *Am J Respir Cell Mol Biol* 2005; 33: 113-120.
5. Selman M, Pardo A. Idiopathic pulmonary fibrosis: an epithelial/fibroblastic cross-talk disorder. *Respir Res* 2002; 3: 3.
6. Thannickal VJ, Toews GB, White ES, Lynch JP, 3rd, Martinez FJ. Mechanisms of pulmonary fibrosis. *Annu Rev Med* 2004; 55: 395-417.
7. Leask A, Abraham DJ. TGF-beta signaling and the fibrotic response. *Faseb J* 2004; 18: 816-827.
8. Leask A, Holmes A, Abraham DJ. Connective tissue growth factor: a new and important player in the pathogenesis of fibrosis. *Curr Rheumatol Rep* 2002; 4: 136-142.
9. Broekelmann TJ, Limper AH, Colby TV, McDonald JA. Transforming growth factor beta 1 is present at sites of extracellular matrix gene expression in human pulmonary fibrosis. *Proc Natl Acad Sci U S A* 1991; 88: 6642-6646.
10. Kaminski N, Allard JD, Pittet JF, Zuo F, Griffiths MJ, Morris D, Huang X, Sheppard D, Heller RA. Global analysis of gene expression in pulmonary fibrosis reveals distinct programs regulating lung inflammation and fibrosis. *Proc Natl Acad Sci U S A* 2000; 97: 1778-1783.
11. Sime PJ, Xing Z, Graham FL, Csaky KG, Gauldie J. Adenovector-mediated gene transfer of active transforming growth factor-beta1 induces prolonged severe fibrosis in rat lung. *J Clin Invest* 1997; 100: 768-776.
12. Santana A, Saxena B, Noble NA, Gold LI, Marshall BC. Increased expression of transforming growth factor beta isoforms (beta 1, beta 2, beta 3) in bleomycin-induced pulmonary fibrosis. *Am J Respir Cell Mol Biol* 1995; 13: 34-44.
13. Phan SH, Kunkel SL. Lung cytokine production in bleomycin-induced pulmonary fibrosis. *Exp Lung Res* 1992; 18: 29-43.
14. Kang HR, Cho SJ, Lee CG, Homer RJ, Elias JA. Transforming growth factor (TGF)-beta1 stimulates pulmonary fibrosis and inflammation via a Bax-dependent, bid-activated pathway that involves matrix metalloproteinase-12. *J Biol Chem* 2007; 282: 7723-7732.
15. Giri SN, Hyde DM, Hollinger MA. Effect of antibody to transforming growth factor beta on bleomycin induced accumulation of lung collagen in mice. *Thorax* 1993; 48: 959-966.
16. Wang Q, Wang Y, Hyde DM, Gotwals PJ, Koteliansky VE, Ryan ST, Giri SN. Reduction of bleomycin induced lung fibrosis by transforming growth factor beta soluble receptor in hamsters. *Thorax* 1999; 54: 805-812.
17. Feng XH, Derynck R. Specificity and versatility in tgf-beta signaling through Smads. *Annu Rev Cell Dev Biol* 2005; 21: 659-693.
18. Derynck R, Zhang YE. Smad-dependent and Smad-independent pathways in TGF-beta family signalling. *Nature* 2003; 425: 577-584.
19. Sandbo N, Dulin N. Actin cytoskeleton in myofibroblast differentiation: ultrastructure defining form and driving function. *Transl Res* 2011; 158: 181-196.

20. Sandbo N, Kregel S, Taurin S, Bhorade S, Dulin NO. Critical role of serum response factor in pulmonary myofibroblast differentiation induced by TGF-beta. *Am J Respir Cell Mol Biol* 2009; 41: 332-338.
21. Sandbo N, Lau A, Kach J, Ngam C, Yau D, Dulin NO. Delayed stress fiber formation mediates pulmonary myofibroblast differentiation in response to TGF-beta. *Am J Physiol Lung Cell Mol Physiol* 2011; 301: L656-666.
22. Conte E, Fruciano M, Fagone E, Gili E, Caraci F, Iemmolo M, Crimi N, Vancheri C. Inhibition of PI3K prevents the proliferation and differentiation of human lung fibroblasts into myofibroblasts: the role of class I P110 isoforms. *PLoS One* 2011; 6: e24663.
23. Fagone E, Conte E, Gili E, Fruciano M, Pistorio MP, Lo Furno D, Giuffrida R, Crimi N, Vancheri C. Resveratrol inhibits transforming growth factor-beta-induced proliferation and differentiation of ex vivo human lung fibroblasts into myofibroblasts through ERK/Akt inhibition and PTEN restoration. *Exp Lung Res* 2011; 37: 162-174.
24. Kulkarni AA, Thatcher TH, Olsen KC, Maggirwar SB, Phipps RP, Sime PJ. PPAR-gamma ligands repress TGFbeta-induced myofibroblast differentiation by targeting the PI3K/Akt pathway: implications for therapy of fibrosis. *PLoS One* 2011; 6: e15909.
25. Bill A, Alex Gaither L. The Mechanistic Role of the Calcium-Activated Chloride Channel ANO1 in Tumor Growth and Signaling. *Adv Exp Med Biol* 2017; 966: 1-14.
26. Crottes D, Jan LY. The multifaceted role of TMEM16A in cancer. *Cell Calcium* 2019; 82: 102050.
27. Caputo A, Caci E, Ferrera L, Pedemonte N, Barsanti C, Sondo E, Pfeffer U, Ravazzolo R, Zegarra-Moran O, Galietta LJ. TMEM16A, a membrane protein associated with calcium-dependent chloride channel activity. *Science* 2008; 322: 590-594.
28. Schroeder BC, Cheng T, Jan YN, Jan LY. Expression cloning of TMEM16A as a calcium-activated chloride channel subunit. *Cell* 2008; 134: 1019-1029.
29. Yang YD, Cho H, Koo JY, Tak MH, Cho Y, Shim WS, Park SP, Lee J, Lee B, Kim BM, Raouf R, Shin YK, Oh U. TMEM16A confers receptor-activated calcium-dependent chloride conductance. *Nature* 2008; 455: 1210-1215.
30. Jang Y, Oh U. Anoctamin 1 in secretory epithelia. *Cell Calcium* 2014; 55: 355-361.
31. Sanders KM, Zhu MH, Britton F, Koh SD, Ward SM. Anoctamins and gastrointestinal smooth muscle excitability. *Exp Physiol* 2012; 97: 200-206.
32. Oh U, Jung J. Cellular functions of TMEM16/anoctamin. *Pflugers Arch* 2016; 468: 443-453.
33. Cho CH, Lee S, Kim A, Yarishkin O, Ryoo K, Lee YS, Jung HG, Yang E, Lee DY, Lee B, Kim H, Oh U, Im HI, Hwang EM, Park JY. TMEM16A expression in cholinergic neurons of the medial habenula mediates anxiety-related behaviors. *EMBO Rep* 2020; 21: e48097.
34. Simchowitz L, De Weer P. Chloride movements in human neutrophils. Diffusion, exchange, and active transport. *J Gen Physiol* 1986; 88: 167-194.
35. Mattes PM, Maloney PC, Littlefield JW. Altered chloride metabolism in cultured cystic fibrosis skin fibroblasts. *Proc Natl Acad Sci U S A* 1987; 84: 3009-3013.
36. Ashcroft T, Simpson JM, Timbrell V. Simple method of estimating severity of pulmonary fibrosis on a numerical scale. *J Clin Pathol* 1988; 41: 467-470.
37. Namkung W, Phuan PW, Verkman AS. TMEM16A inhibitors reveal TMEM16A as a minor component of calcium-activated chloride channel conductance in airway and intestinal epithelial cells. *J Biol Chem* 2011; 286: 2365-2374.
38. Kimura K, Ito M, Amano M, Chihara K, Fukata Y, Nakafuku M, Yamamori B, Feng J, Nakano T, Okawa K, Iwamatsu A, Kaibuchi K. Regulation of myosin phosphatase by Rho and Rho-associated kinase (Rho-kinase). *Science* 1996; 273: 245-248.
39. Birukova AA, Shah AS, Tian Y, Moldobaeva N, Birukov KG. Dual role of vinculin in barrier-disruptive and barrier-enhancing endothelial cell responses. *Cell Signal* 2016; 28: 541-551.

40. Birukova AA, Tian X, Cokic I, Beckham Y, Gardel ML, Birukov KG. Endothelial barrier disruption and recovery is controlled by substrate stiffness. *Microvasc Res* 2013; 87: 50-57.
41. Britschgi A, Bill A, Brinkhaus H, Rothwell C, Clay I, Duss S, Rebhan M, Raman P, Guy CT, Wetzel K, George E, Popa MO, Lilley S, Choudhury H, Gosling M, Wang L, Fitzgerald S, Borawski J, Baffoe J, Labow M, Gaither LA, Bentires-Alj M. Calcium-activated chloride channel ANO1 promotes breast cancer progression by activating EGFR and CAMK signaling. *Proc Natl Acad Sci U S A* 2013; 110: E1026-1034.
42. Liu Z, Zhang S, Hou F, Zhang C, Gao J, Wang K. Inhibition of Ca(2+) -activated chloride channel ANO1 suppresses ovarian cancer through inactivating PI3K/Akt signaling. *Int J Cancer* 2019; 144: 2215-2226.
43. Dulin NO. Calcium-Activated Chloride Channel ANO1/TMEM16A: Regulation of Expression and Signaling. *Front Physiol* 2020; 11: 590262.
44. Wang Q, Bai L, Luo S, Wang T, Yang F, Xia J, Wang H, Ma K, Liu M, Wu S, Wang H, Guo S, Sun X, Xiao Q. TMEM16A Ca(2+)-activated Cl(-) channel inhibition ameliorates acute pancreatitis via the IP3R/Ca(2+)/NFkappaB/IL-6 signaling pathway. *J Adv Res* 2020; 23: 25-35.
45. Eickelberg O, Pansky A, Mussmann R, Bihl M, Tamm M, Hildebrand P, Perruchoud AP, Roth M. Transforming growth factor-beta1 induces interleukin-6 expression via activating protein-1 consisting of JunD homodimers in primary human lung fibroblasts. *J Biol Chem* 1999; 274: 12933-12938.
46. Pedroza M, Le TT, Lewis K, Karmouty-Quintana H, To S, George AT, Blackburn MR, Tweardy DJ, Agarwal SK. STAT-3 contributes to pulmonary fibrosis through epithelial injury and fibroblast-myofibroblast differentiation. *FASEB J* 2016; 30: 129-140.
47. Zhang XH, Zheng B, Yang Z, He M, Yue LY, Zhang RN, Zhang M, Zhang W, Zhang X, Wen JK. TMEM16A and myocardin form a positive feedback loop that is disrupted by KLF5 during Ang II-induced vascular remodeling. *Hypertension* 2015; 66: 412-421.
48. Friard J, Tauc M, Cougnon M, Compan V, Duranton C, Rubera I. Comparative Effects of Chloride Channel Inhibitors on LRRC8/VRAC-Mediated Chloride Conductance. *Front Pharmacol* 2017; 8: 328.
49. Davis AJ, Shi J, Pritchard HA, Chadha PS, Leblanc N, Vasilikostas G, Yao Z, Verkman AS, Albert AP, Greenwood IA. Potent vasorelaxant activity of the TMEM16A inhibitor T16A(inh) -A01. *Br J Pharmacol* 2013; 168: 773-784.

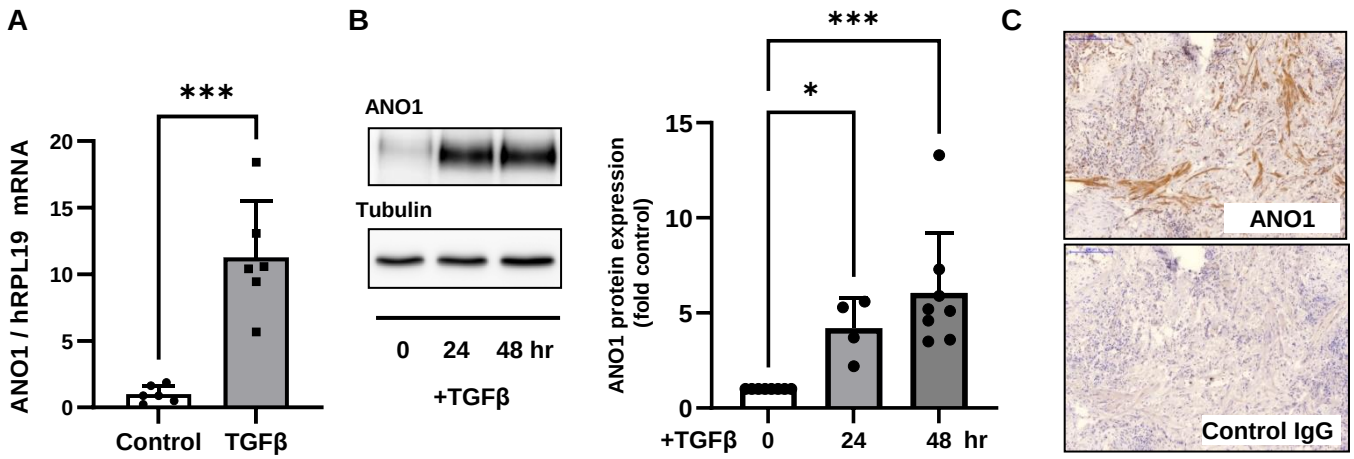

Figure 1. Expression of ANO1 in human lung myofibroblasts and in fibrotic areas of human lungs with idiopathic pulmonary fibrosis (IPF). A-B, Confluent human lung fibroblasts (HLF) were serum starved in 0.1% FBS for 48 hr, followed by treatment with TGF-β (1 ng/ml) for indicated times. A, ANO1 mRNA expression as determined by RT-qPCR. Data are the mean values ±SD. ***p<0.001, t-test. **B,** Representative image and quantitation of ANO1 protein expression as determined by western blot analysis. Data are the normalized to control mean immunoreactivity values ±SD. *, p<0.05, ***p<0.001, Kruskal-Wallis non-parametric test with Dunn's correction for multiple comparisons. **C,** Immunohistochemical staining of fibrotic areas of human IPF lung sequential sections with ANO1 antibodies as compared to the IgG control. Shown are representative IHC images from three IPF lungs.

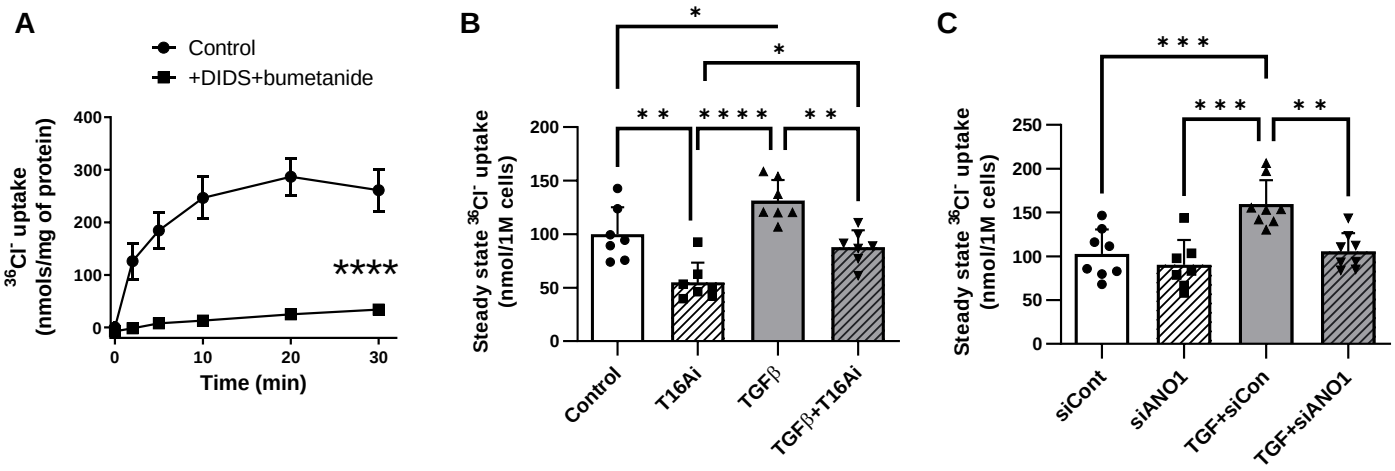

Figure 2. Effect of TGFβ on and the role of ANO1 in a control of intracellular Cl^- levels in human lung fibroblasts (HLF). A, Kinetics of Cl^- accumulation in HLF. Cl^- uptake was measured as radiotracer accumulation after adding $^{36}Cl^-$ into cell culture medium. Serum-starved (for 48 hr) HLF cells were pretreated for 30 min with either vehicle or combination of 1 mM DIDS plus 20 µM bumetanide. The same inhibitors were present in transport assay media. Data are the mean values ±SD in three experiments. ****p<0.0001, repeated measures ANOVA; inhibitors vs. control. **B,** Effect of the ANO1 inhibitor, T16Ainh-A01 (T16Ai), on intracellular Cl^- levels in control and TGF-β-treated HLF. Intracellular Cl^- levels were measured as the steady state $^{36}Cl^-$ accumulation and normalized to the number of cells per well as described in methods. 30 µM T16Ainh-A01 for 1 h before and during $^{36}Cl^-$ transport assay. Data represent the mean values ±SD from seven independent experiments in two HLF passages. *p<0.01, **p<0.01; ***p<0.001; One-way ANOVA with Tukey post hoc correction for multiple comparisons. **C,** The effect of siRNA-mediated ANO1 knockdown on intracellular Cl^- levels in control and TGFβ-treated primary human lung fibroblasts. HLF cells were treated with the siRNA targeting ANO1 (siANO1) or the negative control siRNA (siCont), and TGF-β or vehicle control for 48hr as described in Methods. The steady-state $^{36}Cl^-$ accumulation was measured and normalized as in panel B. Data represent the mean values ±SE of eight independent experiments performed in two HLF passages. **p<0.01, ***p<0.001, One-way ANOVA with Tukey post hoc correction for multiple comparisons.

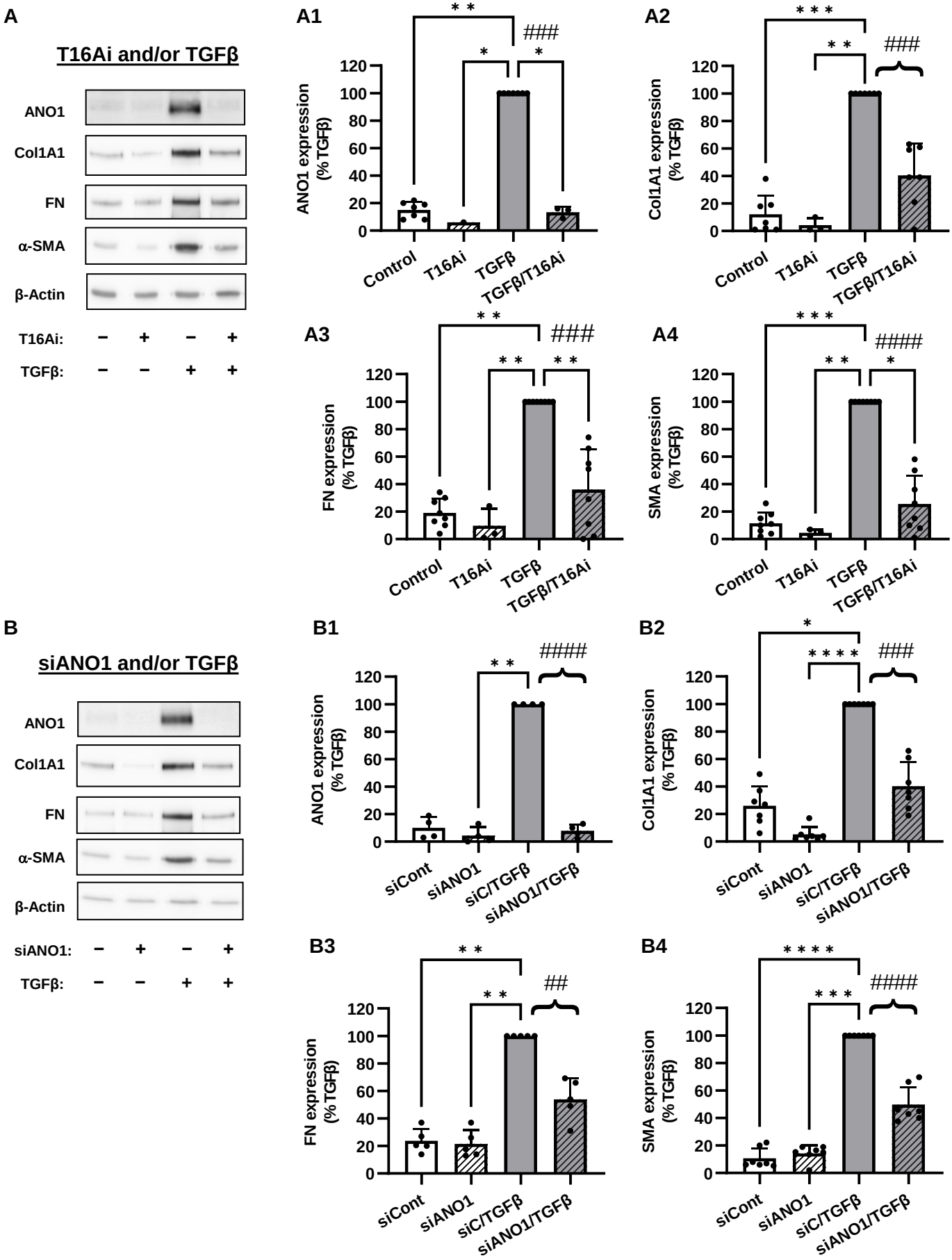
A
T16Ai and/or TGFβ
ANO1
Col1A1
FN
α-SMA
β-Actin
T16Ai: − + − +
TGFβ: − − + +
A1
ANO1 expression (% TGFβ)
A2
Col1A1 expression (% TGFβ)
A3
FN expression (% TGFβ)
A4
SMA expression (% TGFβ)
Control
T16Ai
TGFβ
TGFβ/T16Ai
B
siANO1 and/or TGFβ
ANO1
Col1A1
FN
α-SMA
β-Actin
siANO1: − + − +
TGFβ: − − + +
B1
ANO1 expression (% TGFβ)
B2
Col1A1 expression (% TGFβ)
B3
FN expression (% TGFβ)
B4
SMA expression (% TGFβ)
siCont
siANO1
siC/TGFβ
siANO1/TGFβ

From previous page

Figure 3. Role of ANO1 in TGFβ-induced myofibroblast differentiation.
A, Representative image and quantification of western blot analysis of the effect of the pharmacological inhibitor of ANO1, $T16A_{inh}$-A01 (T16Ai) on myofibroblast differentiation. Serum-starved (48 hr) HLF were pretreated with the T16Ai for 1hr, followed by treatment with TGF-β (1 ng/ml) for 48 hr. Cell lysates were then probed for immunoreactivity of anactomin-1 (ANO1, **A1**), collagen 1A1 (Col1A1, **A2**), fibronectin (FN, **A3**), and smooth muscle α-actin (SMA, **A4**). Data are the mean values ± SD. *p<0.05, **p<0.01, ***p<0.001, Kruskal-Wallis with Dunn's post hoc correction vs. TGFβ group. Brace brackets and $^{###}$p<0.001; $^{####}$, p<0.0001, preplanned comparison of TGF-β effect with and without ANO1 inhibitor.
B, Representative image and quantification of western blot analysis of the effect of siRNA targeting ANO1 on myofibroblast transformation. Serum-starved (48 hr) HLF were treated with ANO1 siRNA followed by treatment with TGF-β (1 ng/ml) for 48 hr. Cell lysates were then probed for immunoreactivity of anactomin-1 (ANO1, **B1**), collagen 1A1 (Col1A1, **B2**), fibronectin (FN, **B3**), and smooth muscle α-actin (SMA, **B4**). Data are the mean values ±SD. *p<0.05, **p<0.01, ***p<0.001, Kruskal-Wallis with Dunn's post hoc correction vs. TGF-β group. Brace brackets and $^{##}$p<0.01; $^{###}$p<0.001; $^{####}$, p<0.0001, preplanned comparison of TGFβ effect with and without ANO1 siRNA.

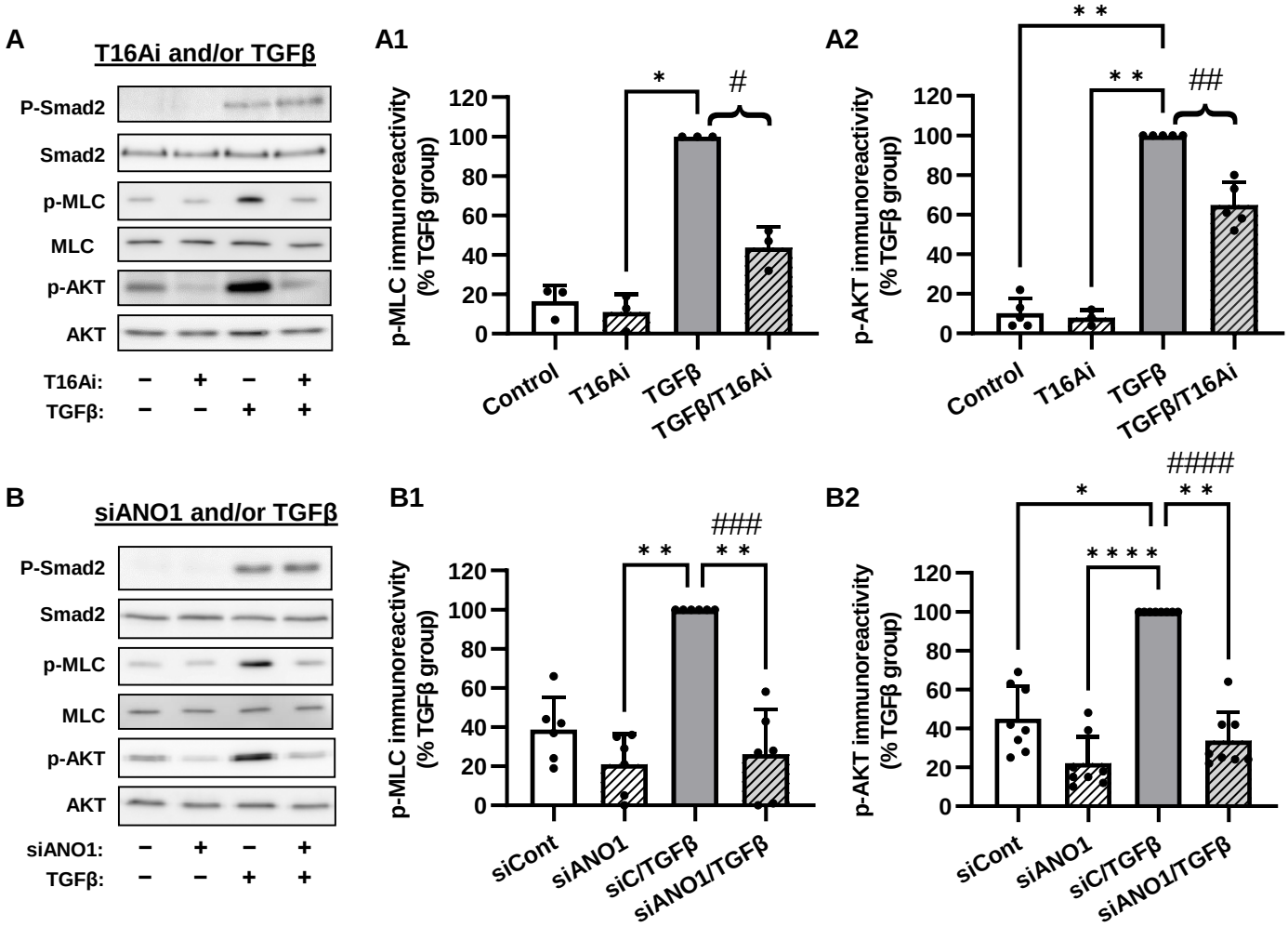

Figure 4. ANO1 controls TGFβ-induced signaling in HLF.

A, Representative image and quantification of western blot analysis of the effect of the pharmacological inhibitor of ANO1, T16Ainh-A01 (T16Ai) on intracellular signaling in HLF. Serum-starved (48 hr) cells were pretreated for 1 hr with T16Ai followed by treatment with TGFβ (1 ng/ml) for 30 minutes (P-Smad2, Smad2), or for 48hr (P-MLC, MLC, P-AKT, AKT). Data represent the mean values of P-MLC (**A1**) and P-AKT (**A2**) immunoreactivity normalized to TGFβ group. *p<0.05, **p<0.01, Kruskal-Wallis with Dunn's post hoc correction vs. TGF-β group. Brace brackets and #p<0.05; ##, p<0.01, preplanned comparison of TGFβ effect with and without T16Ai.

B, Representative image and quantification of western blot analysis of the effect of siRNA targeting ANO1, (siANO1) and nonsense control siRNA (siCont) on intracellular signaling in HLF. Cells were transfected with siCont or siANO1, serum-starved (48 hr), followed by treatment with TGF-β (1 ng/ml) for 30 minutes (P-Smad2, Smad2), or for 48hr (P-MLC, MLC, P-AKT, AKT). Data represent the mean values of P-MLC (**B1**) and P-AKT (**B2**) immunoreactivity normalized to TGFβ group. *p<0.05, **p<0.01, 888p<0.001, ****p<0.0001, Kruskal-Wallis with Dunn's post hoc correction vs. TGF-β group. ###p<0.001, ####p<0.01, preplanned comparison of TGFβ effect with and without siANO1.